Journal of Nondestructive Evaluation (2019) 38:54
https://doi.org/10.1007/s10921-019-0591-8

A Comprehensive Study on Detection of Hidden Delamination Damage in a Composite Plate Using Curvatures of Operating Deflection Shapes

Da-Ming Chen[1] · Y. F. Xu[2] · W. D. Zhu[1]

Received: 3 July 2018 / Accepted: 9 April 2019 / Published online: 29 April 2019

Abstract

The aim of this work is to investigate the accuracy and sensitivity of a continuously scanning laser Doppler vibrometer (CSLDV) for detection of hidden delamination damage in composite plates. Some work on using a CSLDV for detection of damage in aluminum beams and plates has been done by the authors. The current work is related to a worldwide round robin study sponsored by the Society of Experimental Mechanics. The main difference between the current work and previous work is that the damaged composite plate was provided by the organizer of the round robin study instead of being made by the authors. Hence, the authors have no information about locations of the damage, which means this is more like a blind test. The most significant advantage of using a CSLDV for vibration measurement of a structure is that a spatially dense operating deflection shape (ODS) of the structure can be obtained and further used to calculate the curvature of the ODS (CODS). A comprehensive study to detect the hidden damage in the composite plate by using the first seven CODSs from the corresponding ODSs of the plate is conducted. The study shows that different CODSs have different sensitivities to local anomaly induced by the damage and only two of the seven CODSs can be used to detect the locations of the hidden damage.

Keywords Composite · Delamination · Continuously scanning laser Doppler vibrometer · Curvature of operating deflection shape

1 Introduction

Composites have been widely used in many modern engineering structures due to their high specific stiffness and strength [1]. However, presence of damage, such as delamination between plies, can severely degrade stiffness and strength of composites and cause catastrophic structural failure. Furthermore, anisotropic material properties of composites and the fact that much of damage in composites occurs beneath a surface of laminates increase the difficulty in detecting damage in composites [2]. Hence, development of a reliable and effective nondestructive damage detection method is important to maintain safety and integrity of a composite structure.

Since damage-induced changes in physical properties of a structure can cause detectable changes in modal characteristics of the structure, vibration-based damage detection methods have attracted much attention and become a major research topic of structural dynamics [3,4]. Valdes and Soutis [5] investigated the effect of delamination on natural frequencies of laminated composite beams. They found that changes of the natural frequencies of beams after delamination give a good indication of severity of damage. Qiao et al. [6] used a surface-bonded piezoelectric sensor system and a non-contact scanning laser Doppler vibrometer (SLDV) to measure dynamic response of laminated composite beams. They applied three curvature-based damage detection algorithms to measurement data from the two sensor systems and detected different types of damage in the composite beams. Later, the two sensor systems and three damage detection algorithms were used to detect delamination in laminated composite plates [7]. Lestari et al. [8] derived the governing

✉ W. D. Zhu
wzhu@umbc.edu

Da-Ming Chen
damingc1@umbc.edu

Y. F. Xu
xu2yf@ucmail.uc.edu

1 Department of Mechanical Engineering, University of Maryland, Baltimore County, 1000 Hilltop Circle, Baltimore, MD 21250, USA

2 Department of Mechanical and Materials Engineering, University of Cincinnati, Cincinnati, OH 45221, USA

equation of a damaged beam by assuming the effect of damage as stiffness loss. They used surface-bonded piezoelectric sensors to directly obtain curvature mode shapes and detect different types of damage in laminated composite beams. He et al. [9] conducted modal analysis on undamaged and damaged composite beams with single and multiple damage with different severity. They used curvature mode differences to identify damage and found that they increase with the number of delamination. Besides the methods mentioned above for composite structures, methods using signal processing, such as a two-dimensional (2D) wavelet transform, are also applied to detect damage in composite structures [10–13]. Fan and Qiao [14] proposed a damage detection algorithm using the Dergauss2d wavelet and applied it to detect impact damage in a composite plate. Compared with the 2D strain energy method [15] and 2D gapped smoothing method [16], they found that their proposed algorithm is superior in noise immunity and robust with limited sensor data. Yang and Oyadiji [17] proposed a damage detection approach using a modal frequency surface, which is generated by attaching a point mass at different locations of a structure, and its wavelet coefficients are calculated. They found that the wavelet coefficients can characterize locations and shapes of both near and far surface delamination in laminated composite plates. Xu et al. [18] used complex-wavelet 2D curvature mode shapes to detect small-sized delamination in carbon fiber reinforced polymer laminated plates under noisy conditions. They found that the complex-wavelet 2D curvature mode shapes have stronger damage sensitivities and noise robustness than conventional 2D curvature mode shapes.

A SLDV has been widely used in the vibration community because it provides non-contact and spatially dense velocity measurement [19–21]. In conventional vibration analysis with use of a SLDV, a structure surface is divided by a grid and the laser spot from the SLDV stays at a point long enough to measure time-domain velocity response of the point and then moves to the next one; this is called stepped scanning and it is a conventional fixed sensor measurement technique. After all the points on the grid are measured, Fourier transform is applied to time-domain velocity response of each point and an operating deflection shape (ODS) of the structure is obtained. Spatial resolution of the ODS obtained by this fixed sensor measurement technique is usually good enough for vibration analysis. However, when the ODS is used for detection of small-sized damage, it may require much denser spatial resolution to capture local anomaly induced by the small-sized damage. Since the curvature of an ODS (CODS), i.e., the second-order spatial derivative of an ODS, is more sensitive to damage than the ODS [22], curvature-based methods have been widely applied to damage detection. As mentioned above, an ODS from the fixed sensor measurement technique is obtained by Fourier transform of time-domain velocity response. Based on properties of Fourier transform, high-frequency noise components in the ODS are amplified after its second-order differentiation operation [23], which can reduce effectiveness of the curvature-based methods on damage detection. Hence, many signal processing methods, including a 2D wavelet transform, are proposed to reduce the adverse effect of measurement noise on damage detection. In this work, a real-time moving sensor, i.e., a continuously SLDV (CSLDV), is used for damage detection. A CSLDV can achieve a function that its laser spot continuously moves on a structure surface along a scan trajectory [24]. There are two advantages to use a CSLDV for damage detection. The first one is that spatial resolution of an ODS is much denser since the laser spot can measure all the points along the scan trajectory, which can increase the possibility to capture local anomaly induced by small-sized damage. The second one is that a completely different data processing method, i.e., the demodulation method [25], is used to obtain an ODS from velocity response measured by a CSLDV, which does not involve Fourier transform.

A focus group on SLDV methods and applications met at the 2017 International Modal Analysis Conference organized by the Society of Experimental Mechanics and decided to have a round robin study on detection of damage in a composite plate; the start date of the study is July 2017. The composite plate being studied has 20 plies and the size of the plate is 300 mm × 100 mm with a thickness of 2.5 mm; it was manufactured by the organizer of the focus group and round robin study at the University of Bristol in the UK. Two damage in the form of two cuts was introduced on the 10th and 11th plies and their sizes are 15 mm × 15 mm and 5 mm × 5 mm. The 15 mm × 15 mm cut was then filled with one layer of kitchen foil. No damage can be seen from appearance inspection. Five groups of researchers in Europe and the U.S. were involved in the study. Without knowing damage locations beforehand for the researchers, their goal is to detect the damage locations with use of any SLDV method. This round robin study provides a good opportunity to investigate the accuracy and sensitivity of a CSLDV in detection of hidden damage in composite plates, which would be a good application for the CSLDV.

Some work on using a CSLDV for detection of damage in aluminum beams and plates has been done by the authors [26–28]. The current work to detect the hidden delamination damage in the composite plate uses the same damage detection methodology as that in [28]. More efforts taken in the current work are to investigate sensitivities of different CODSs of the composite plate to the local anomaly induced by the hidden damage. The effect of spatial resolution of an ODS on detection of small-sized damage is also investigated in this work. In the previous work, there was no discussion about the priority between the scan frequency and number of multiple scans, while the current work tries to give a more detailed investigation on this topic.

2 Methodology

2.1 Design of a CSLDV

To achieve the function that the laser spot from a CSLDV continuously moves on a structure surface and measures velocity response, three components are needed [29], including a single-point laser Doppler vibrometer, a scanner with X and Y scan mirrors, and a control unit. For a commercial SLDV, such as a Polytec-500 SLDV with an internal scanner, one can directly give continuous signals to scan mirrors to achieve continuous scanning. However, since a commercial SLDV is only used with stepped scanning by default, one has to connect the internal scanner to an external signal generator to achieve continuous scanning, which requires knowledge about specifications of the scanner and pin configuration. A more economic and reliable way is to build an in-house CSLDV through a combination of the three individual components mentioned above. The CSLDV built by the authors includes a Polytec OFV-353 single-point laser Doppler vibrometer, a Cambridge 6240H scanner, and a dSPACE MicroLabBox control unit, as shown in Fig. 1. The individual vibrometer was originally put on a tripod for use, as shown in Fig. 2a. In order to accommodate the scanner and its servo boards on the same tripod, a base plate, a scanner mounting plate, and a vibrometer mounting plate are designed, as shown in Fig. 2b. Two requirements are considered to determine sizes of those plates and their relative positions. The first requirement is to ensure that the gravity center of the CSLDV is close to the center of the tripod head mount plate since the scanner is as heavy as the vibrometer. The second requirement is to ensure that the laser beam from the vibrometer passes through the center of each mirror on the scanner. After the two requirements are satisfied, the sizes of those plates are optimized to reduce their weights. A final design of the CSLDV is shown in Fig. 2c, where the whole CSLDV can be firmly mounted on the tripod. An in-house built CSLDV can reduce equipment cost and increase flexibility for vibration measurement.

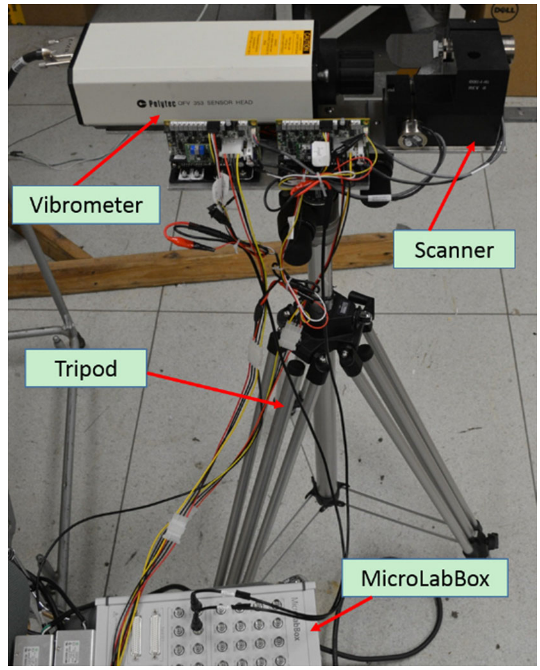

Fig. 1 In-house CSLDV built by the authors

2.2 2D Continuous Scan Scheme

A 2D continuous scan scheme introduced in [28] is used in this work to scan the composite plate, as shown in Fig. 3. The laser spot begins to move from point P_{ll} and simultaneously sweep in right and upward directions until reaching point P_{r2}, which finishes one scan of line $P_{ll}P_{r2}$. If multiple scans for a line are required, the laser spot sweeps back to point P_{ll} and repeats the same scan process between points P_{ll} and P_{r2} until the multiple scans are finished. At the time when the multiple scans for line $P_{ll}P_{r2}$ are finished, the laser spot is at point P_{r2} and continues to simultaneously sweep in left and upward directions until reaching point P_{l2}, which finishes one scan of line $P_{r2}P_{l2}$. The laser spot repeats the above scan process for each scan line and finally reaches point P_{ur} to finish the 2D continuous scan scheme. The corresponding 2D scan trajectory is called a horizontally 2D moving scan trajectory. Details for obtaining corresponding input signals of the scan mirrors can be found in [28]. Velocity response measured by the CSLDV along the 2D continuous scan scheme includes both time- and spatial-domain information, which requires a different signal processing method to obtain an ODS of the composite plate. The demodulation method is applied to obtain the ODS from velocity response and its Fourier transform is not needed. Details of the demodulation method can be found in [28].

2.3 Damage Detection Using CODSs

A curvature-based method is an efficient method to detect damage. The most significant advantage of using a CSLDV for vibration measurement of a structure is that a spatially dense ODS of the structure can be obtained by the demodulation method and further used to calculate the CODS. While an ODS of the composite plate is obtained by the demodulation method from CSLDV measurement, the ODS of the associated undamaged plate can be obtained using polynomials to fit the ODS from the demodulation method [28]. CODSs of the damaged composite plate and associated undamaged plate can then be calculated from the ODSs obtained before. Damage detection can be achieved by using a curvature damage index (CDI) that can distinguish differences between

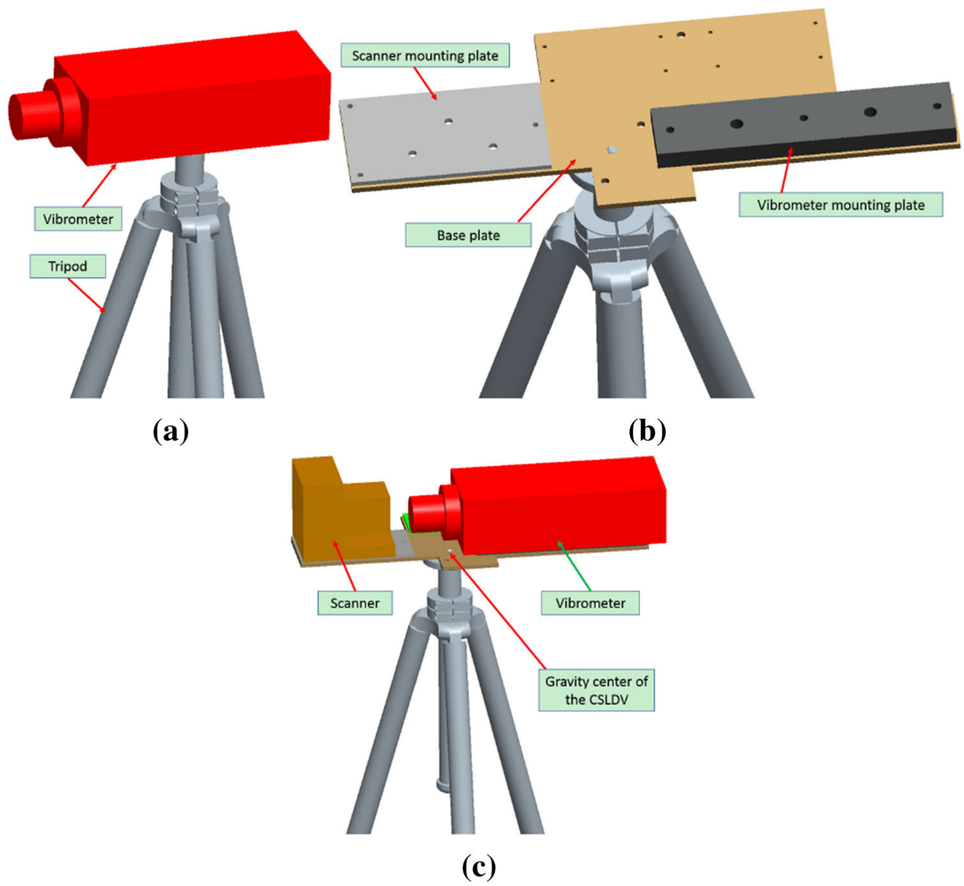

Fig. 2 **a** Individual vibrometer on the tripod by default, **b** three plates designed for the CSLDV, and **c** the CSLDV on the tripod with the aid of the three plates

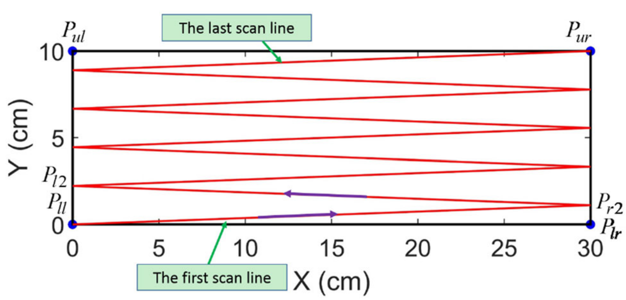

Fig. 3 2D continuous scan scheme for a plate

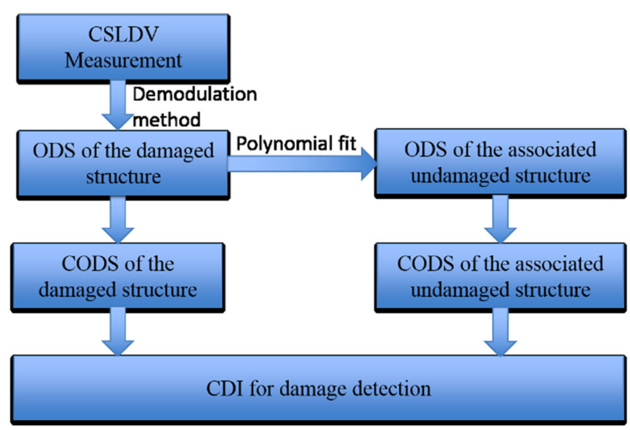

Fig. 4 Flow chart of using a CSLDV for damage detection

the CODSs of the damaged composite plate and associated undamaged plate. Further, a normalized average CDI [28] can be used to assist estimation of the damage size by combining CDIs at different excitation frequencies. A flow chart of using a CSLDV for damage detection is shown in Fig. 4.

3 Round Robin Study

As previously mentioned, the size of the damaged composite plate being studied is 300 mm × 100 mm; the thickness of the plate is 2.5 mm and there are 20 plies along its thickness. The surface of one side of the plate is rough and that of the other side is shinny, as shown in Fig. 5a and b, respectively. No damage can be seen from appearance inspection on both sides. Since the weight of the plate is only 4.54 g and the methodology here is applicable to all boundary conditions of the plate, the authors uses a bench vice to clamp the middle part of the left short edge of the plate, as shown in Fig. 6a. Since stiffness of the plate is large, the clamp area is small to ensure measurable response of the plate by a CSLDV. A retroreflective tape is attached on the shinny surface of the

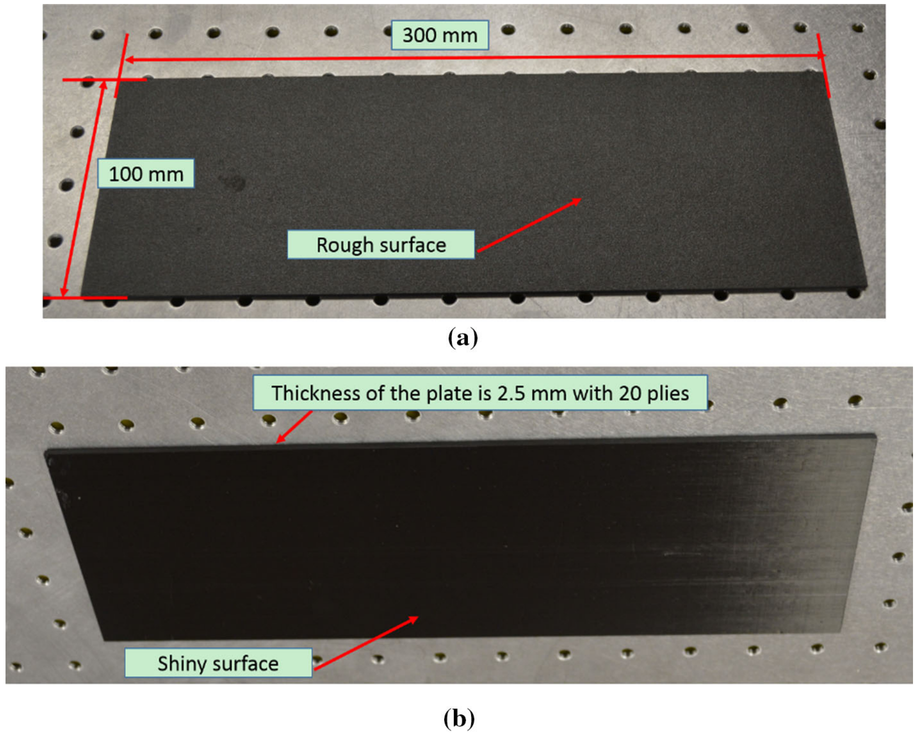

Fig. 5 **a** Rough surface of the damaged composite plate with its length and width dimensions and **b** the shiny surface of the plate with its thickness dimension

plate to enhance laser reflection. Since nondestructive methods must be used in this round robin study, instead of using a shaker that must be attached to the plate, the plate is excited by a speaker [30,31] close to the rough surface of the plate in a non-contact manner, as shown in Fig. 6b. Unlike a shaker or a lead–zirconate–titanate actuator, acoustic excitation by the speaker can avoid any mechanical contact with the composite plate. Hence, there is no external mass or stiffness loading effect on the composite plate.

An impact test is first conducted on the damaged composite plate in Fig. 6a to measure its first seven natural frequencies. A PCB 086C03 impact hammer and the CSLDV are used to excite the plate at an impact point and measure its velocity response at a measurement point, respectively. The first seven natural frequencies, i.e., 29.3 Hz, 82.03 Hz, 199.22 Hz, 297.27 Hz, 563.67 Hz, 1040.23 Hz, and 1777.73 Hz, are used as sinusoidal excitation frequencies. One can see that the seven excitation frequencies cover a frequency range from low-order modes of the plate to its high-order modes, which can provide sufficient data of ODSs, CODSs, and CDIs to detect possible damage locations.

In order to obtain a densest ODS of the damaged composite plate that hardware of the CSLDV can achieve, the composite plate is divided into two scan areas by a middle horizontal line along the long edge direction of the plate. The two scan areas are defined as scan areas 1 and 2, as shown in Fig. 6a. Either scan area is scanned by a horizontally 2D moving scan trajectory, which is similar to that in Fig. 3. Either scan area is formed by 59 scan lines and the number of multiple scans for each scan line is 9. Scan and sampling frequencies of the CSLDV are 0.05 Hz and 10,000 Hz, respectively. The total time to finish a scan of either scan area is 5310 s and the total number of data acquired is $5310 \times 10{,}000 = 53{,}100{,}000$, which is close to the maximum number of data that the hardware can store in one scan. Based on the above parameters, a partial ODS of the plate corresponding to either scan area has a total number of $100{,}000 \times 59 = 5{,}900{,}000$ measurement points and a full ODS of the plate has a total number of $5{,}900{,}000 \times 2 = 11{,}800{,}000$ measurement points. Such dense measurement grids can increase the possibility to capture local anomaly induced by small-sized damage.

3.1 ODSs, CODSs, and CDIs at Different Excitation Frequencies

3.1.1 Excitation Frequency of 29.3 Hz

Partial ODSs of the damaged composite plate corresponding to scan areas 1 and 2 at the excitation frequency of 29.3 Hz obtained by the demodulation method are shown in Fig. 7a and b, respectively. One can see that they are smooth and similar to each other. The full ODS of the plate is formed by the two partial ODSs, as shown in Fig. 7c, and it corresponds to the first mode of the plate, which is a pure bending mode along its long edge direction. Corresponding partial CODSs of scan areas 1 and 2 are shown in Fig. 8a and b, respectively. Unlike the smooth ODSs in Fig. 7, the CODSs have many

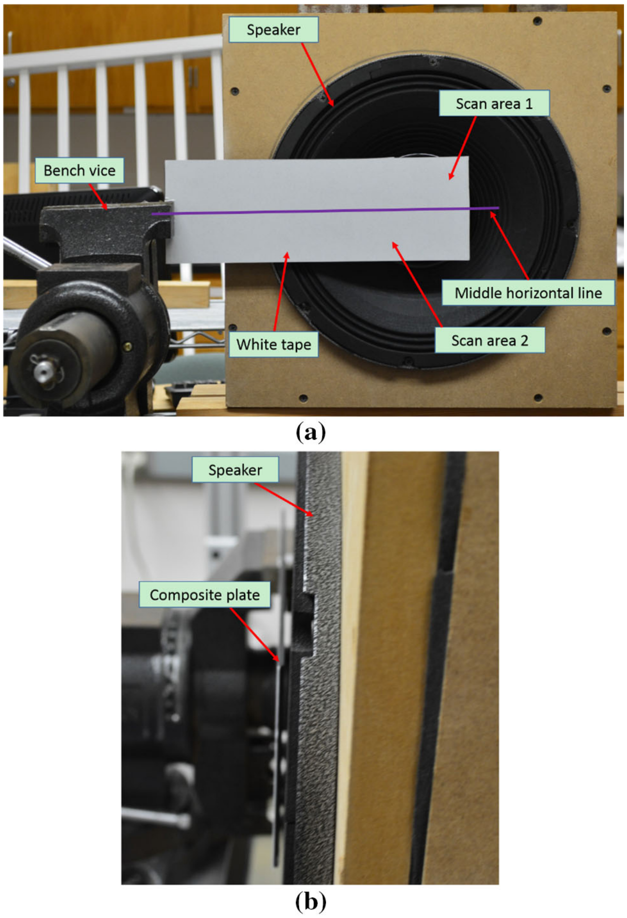

Fig. 6 **a** Experimental setup for detection of damage in the composite plate and **b** non-contact excitation by the speaker

small peaks and it is difficult to see their clear shapes. The ODS and CODS along the first scan line of the 2D scan trajectory in scan area 1 are extracted, as shown in Fig. 9a and b, respectively. One can see that the ODS along the scan line is smooth and has a clear shape. However, the corresponding CODS along the scan line does not have a clear shape. Similar observation can be found from ODSs and CODSs along other scan lines. Corresponding partial CDIs for scan areas 1 and 2 are shown in Fig. 10a and b, respectively. One can see that there are some scattered small areas on the right side of either scan area that have high CDI values. It is difficult to tell whether there is damage in those small areas based on the CDIs at a single excitation frequency.

3.1.2 Excitation Frequency of 82.03 Hz

The full ODS of the damaged composite plate at the excitation frequency of 82.03 Hz is shown in Fig. 11, which is formed by two partial ODSs corresponding to scan areas 1 and 2. One can see that the full ODS of the plate corresponding to its second mode is also a pure bending mode along the long edge direction of the plate. Corresponding partial CODSs of scan areas 1 and 2 are shown in Fig. 12a and b, respectively. Similar to the case at the excitation frequency of 29.3 Hz, it is not easy to distinguish clear shapes of the CODSs in Fig. 12 either. Corresponding partial CDIs for scan areas 1 and 2 are shown in Fig. 13a and b, respectively. The number of scattered small areas with high CDI values on the right side of either scan area is much fewer than that at the excitation frequency of 29.3 Hz. Also, there are no common areas with consistently high CDI values between the CDIs corresponding to the first and second modes of the plate in Figs. 10 and 13, respectively. Hence, the scattered small areas with high CDI values at the excitation frequencies of 29.3 Hz and 82.03 Hz in Figs. 10 and 13, respectively, can be caused by measurement noise.

3.1.3 Excitation Frequency of 199.22 Hz

The full ODS of the damaged composite plate at the excitation frequency of 199.22 Hz is shown in Fig. 14, which is formed by two partial ODSs corresponding to scan areas 1 and 2. One can see that the full ODS of the plate corresponding to its third mode is another pure bending mode along the long edge direction of the plate. Compared with the full ODSs corresponding to the first two pure bending modes at the excitation frequencies of 29.3 Hz and 82.03 Hz, the full ODS at this excitation frequency has more bending variation. Corresponding partial CODSs of scan areas 1 and 2 are shown in Fig. 15a and b, respectively. Shapes of the CODSs can be clearly distinguished and the adverse effect of measurement noise on them is small. The ODS and CODS along the first scan line of the 2D scan trajectory in scan area 1 are extracted, as shown in Fig. 16a and b, respectively. One can see that shapes of both the ODS and CODS are clear. Corresponding partial CDIs for scan areas 1 and 2 are shown in Fig. 17a and b, respectively. An area with high CDI values can be clearly seen in Fig. 17a and CDI values in remaining areas are small, which indicate one possible damage location corresponding to the area with high CDI values. A narrow strip area with high CDI values can also be seen in Fig. 17b, which can be another possible damage location. However, the strip area in Fig. 17b is not as obvious as the area in Fig. 17a since there are some other small areas with somewhat lower CDI values in Fig. 17b. Locations of two possible damage are obtained from the CDIs at this excitation frequency, which are consistent with the information about the number of damage in this round robin study. In order to confirm the damage locations, CDIs at more excitation frequencies are needed.

3.1.4 Excitation Frequency of 297.27 Hz

The full ODS of the damaged composite plate at the excitation frequency of 297.27 Hz is shown in Fig. 18, which is

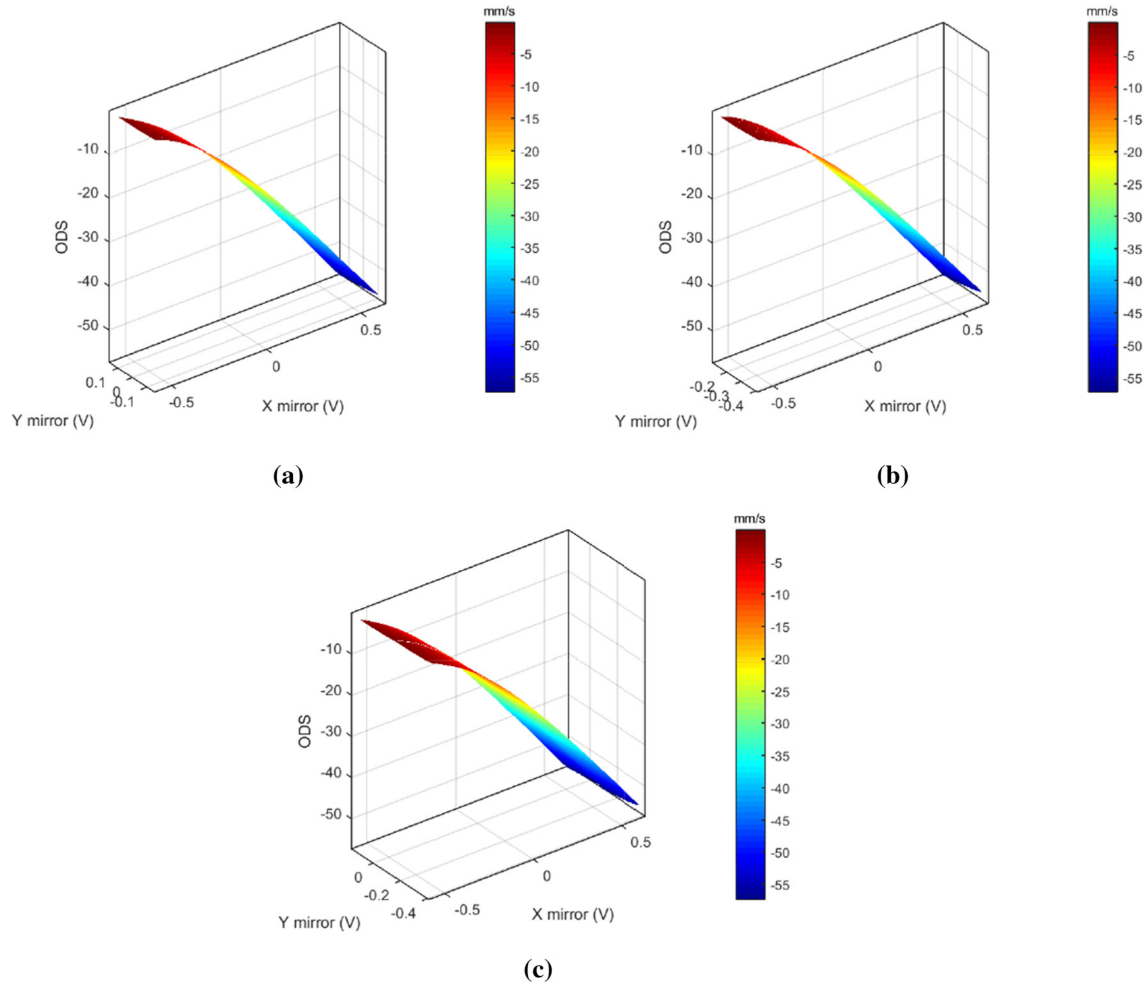

Fig. 7 Partial ODSs corresponding to scan areas **a** 1 and **b** 2; the full ODS of the damaged composite plate is shown in (**c**). All the ODSs are at the excitation frequency of 29.3 Hz

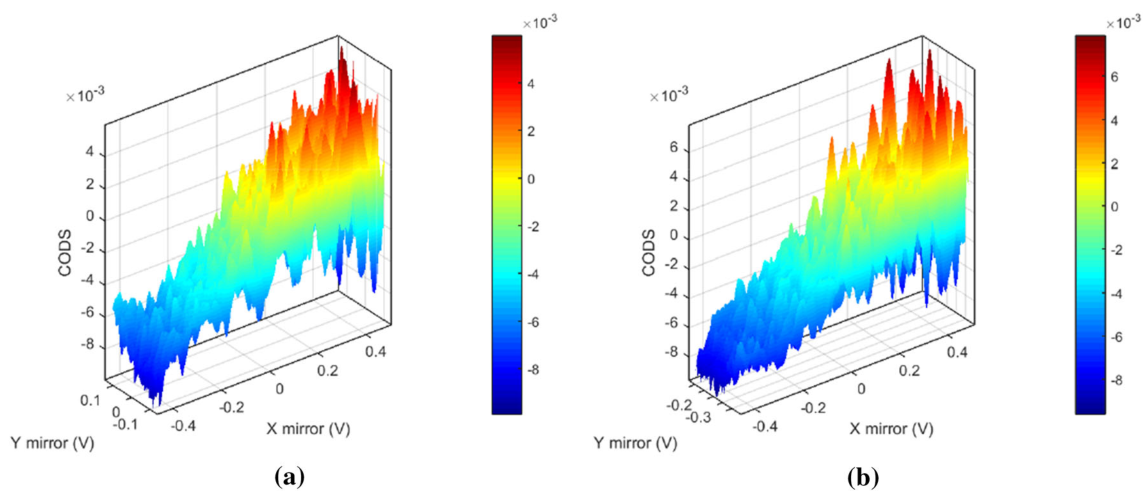

Fig. 8 Corresponding partial CODSs of scan areas **a** 1 and **b** 2 at the excitation frequency of 29.3 Hz

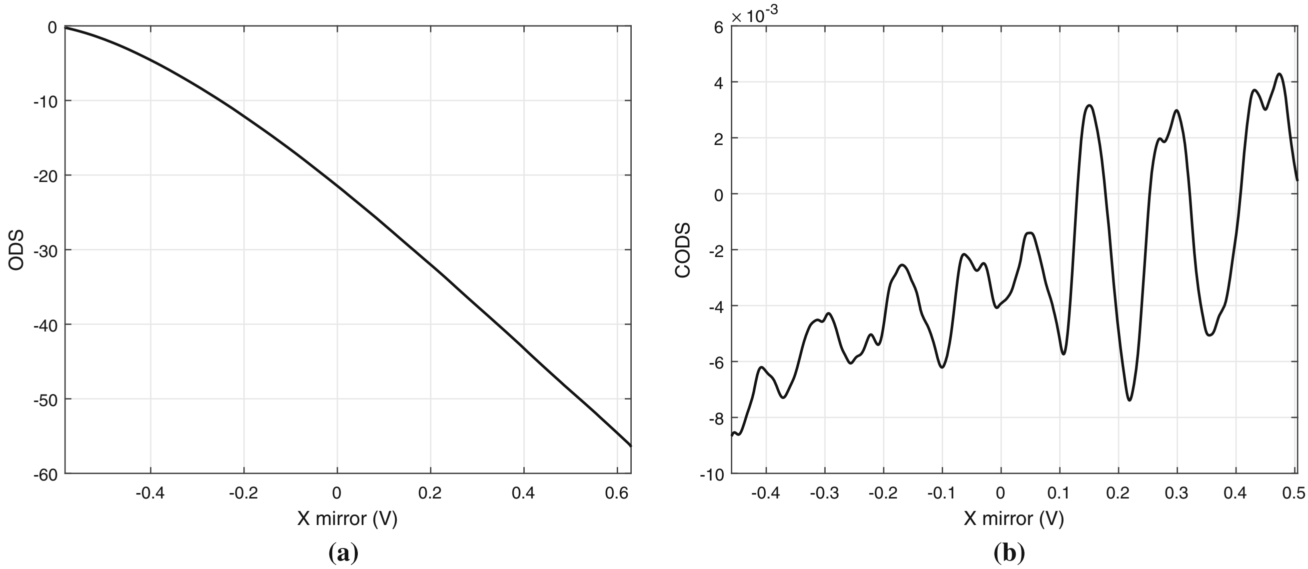

Fig. 9 **a** ODS and **b** CODS along the first scan line of the 2D scan trajectory in scan area 1 at the excitation frequency of 29.3 Hz

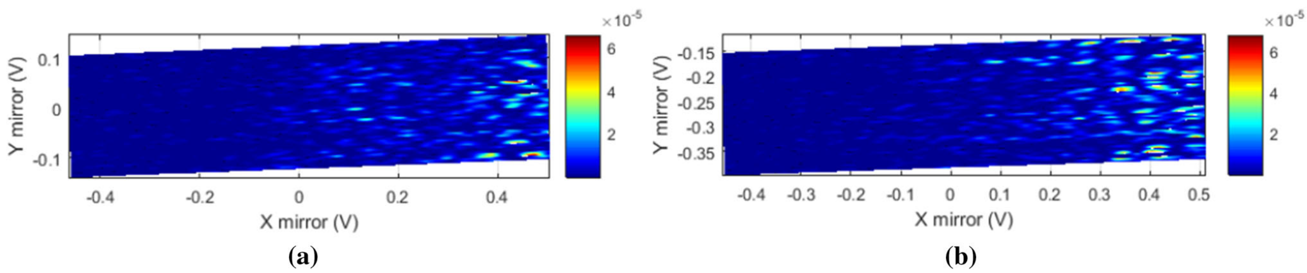

Fig. 10 Corresponding partial CDIs for scan areas **a** 1 and **b** 2 at the excitation frequency of 29.3 Hz

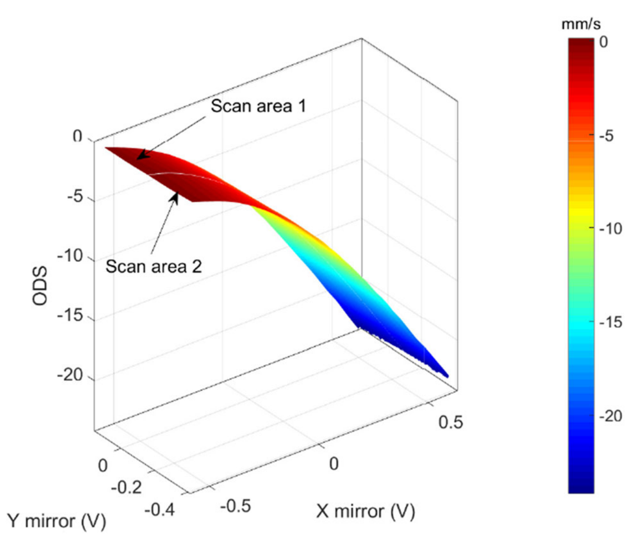

Fig. 11 Full ODS of the damaged composite plate at the excitation frequency of 82.03 Hz

formed by two partial ODSs corresponding to scan areas 1 and 2. One can see that the full ODS of the plate corresponding to its fourth mode is a coupled bending-bending mode along both long and short edge directions of the plate, which is different from the first three pure bending modes of the plate that are only along its long edge direction. Corresponding partial CODSs of scan areas 1 and 2 are shown in Fig. 19a and b, respectively. One can see that shapes of the CODSs are more clear than those at the excitation frequencies of 29.3 Hz and 82.03 Hz, but less clear than those at the excitation frequencies of 199.22 Hz. Corresponding partial CDIs for scan areas 1 and 2 are shown in Fig. 20a and b, respectively. There are no areas with high CDI values on the right side of each scan area in Fig. 20, which indicates that the small areas with high CDI values on the right side of either scan area in Figs. 10 and 13 can be caused by measurement noise. CDI values in Fig. 20a and b at the two possible damage locations obtained from Fig. 17 are small. Hence, CDIs at this excitation frequency cannot be used for detection of damage locations.

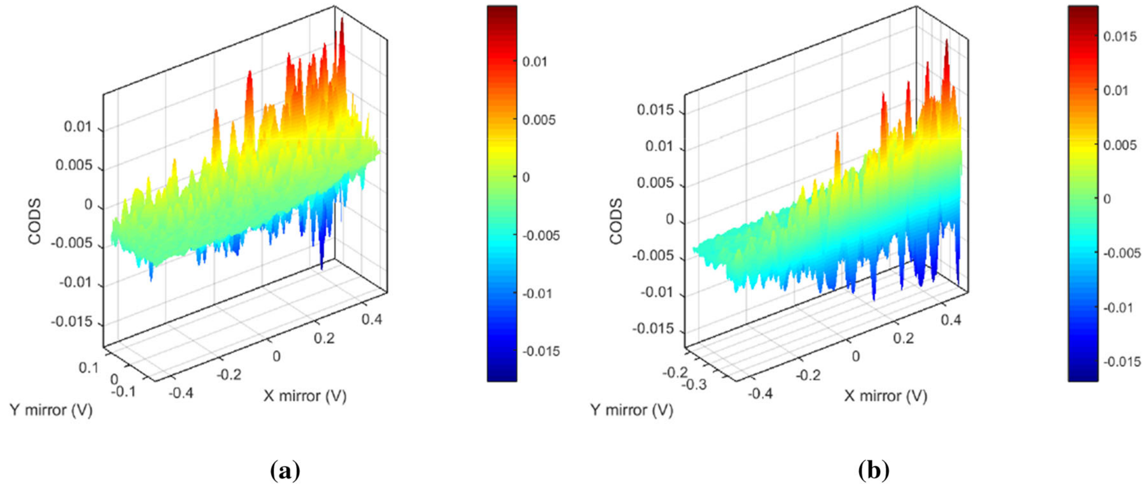

Fig. 12 Corresponding partial CODSs of scan areas **a** 1 and **b** 2 at the excitation frequency of 82.03 Hz

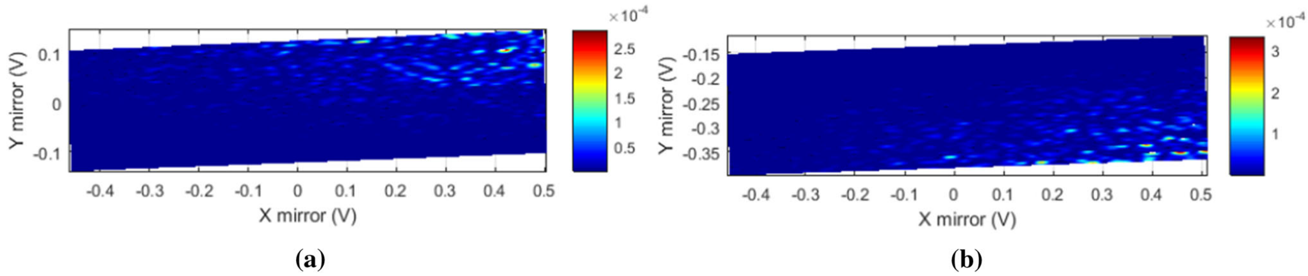

Fig. 13 Corresponding partial CDIs for scan areas **a** 1 and **b** 2 at the excitation frequency of 82.03 Hz

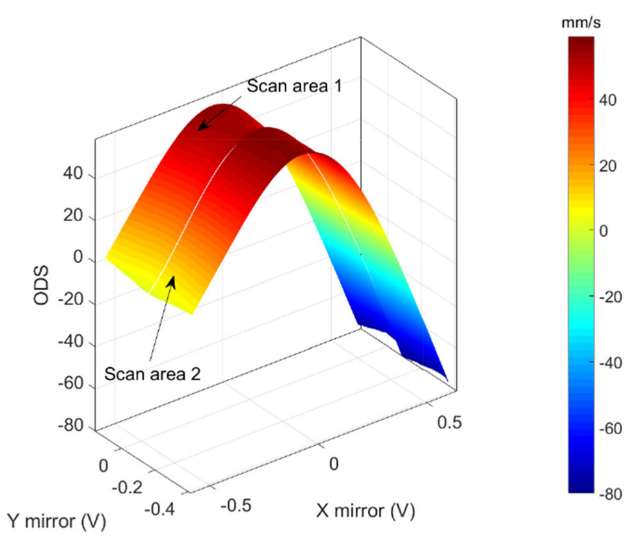

Fig. 14 Full ODS of the damaged composite plate at the excitation frequency of 199.22 Hz

3.1.5 Excitation Frequency of 563.67 Hz

The full ODS of the damaged composite plate at the excitation frequency of 563.67 Hz is shown in Fig. 21, which is formed by two partial ODSs corresponding to scan areas 1 and 2. One can see that the full ODS of the plate corresponding to its fifth mode is another pure bending mode along the long edge direction of the plate. Corresponding partial CODSs of scan areas 1 and 2 are shown in Fig. 22a and b, respectively. Shapes of the CODSs can be clearly distinguished and the effect of measurement noise on them is small. Corresponding partial CDIs for scan areas 1 and 2 are shown in Fig. 23a and b, respectively. One can see that two similar areas with high CDI values to those in Fig. 17 are clearly seen at the two possible damage locations there. Hence, consistently high CDI values are seen at the two possible damage locations at the excitation frequencies of 199.22 Hz and 563.67 Hz, which increases the probability of damage existence at those two locations.

3.1.6 Excitation Frequency of 1040.23 Hz

The full ODS of the damaged composite plate at the excitation frequency of 1040.23 Hz is shown in Fig. 24, which is formed by two partial ODSs corresponding to scan areas 1 and 2. One can see that the full ODS of the plate corresponding to its sixth mode is also a coupled bending-bending mode along both long and short edge directions of the plate. Corresponding partial CODSs of scan areas 1 and 2 are shown

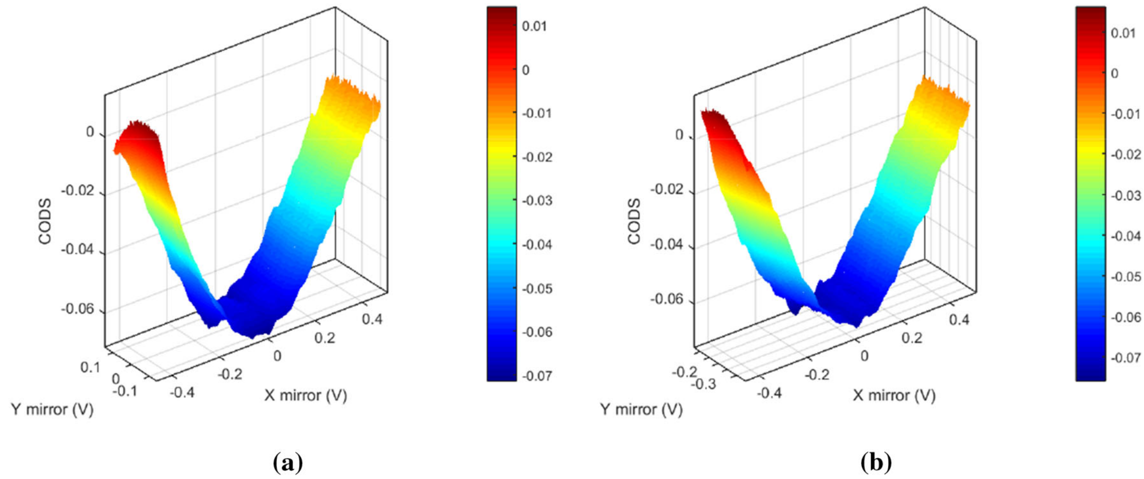

Fig. 15 Corresponding partial CODSs of scan areas **a** 1 and **b** 2 at the excitation frequency of 199.22 Hz

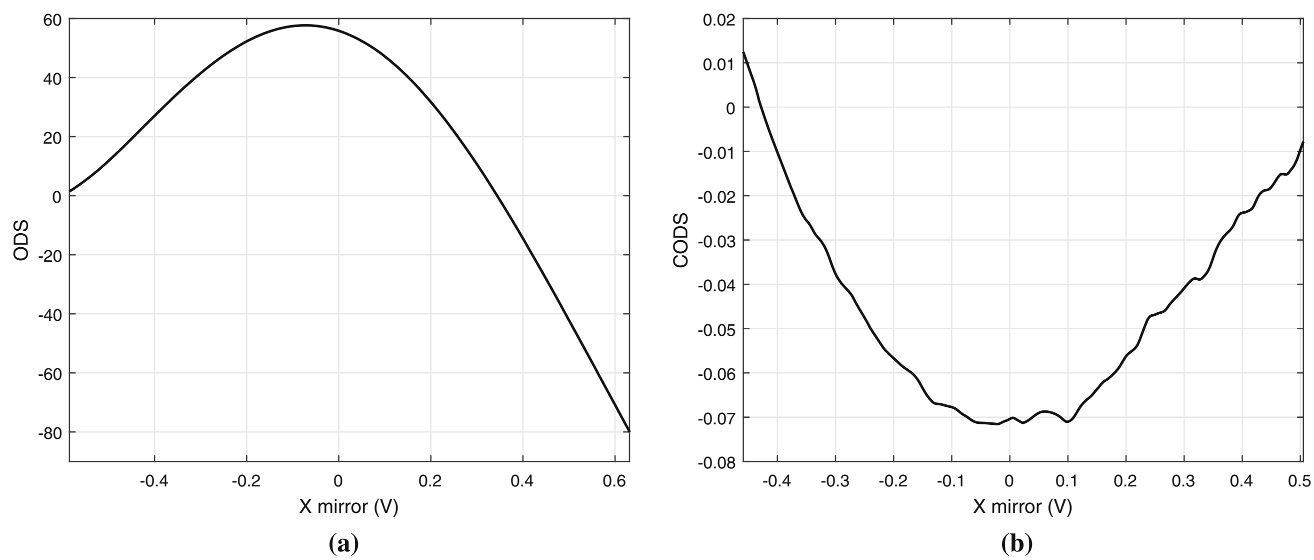

Fig. 16 **a** ODS and **b** CODS along the first scan line of the 2D scan trajectory in scan area 1 at the excitation frequency of 199.22 Hz

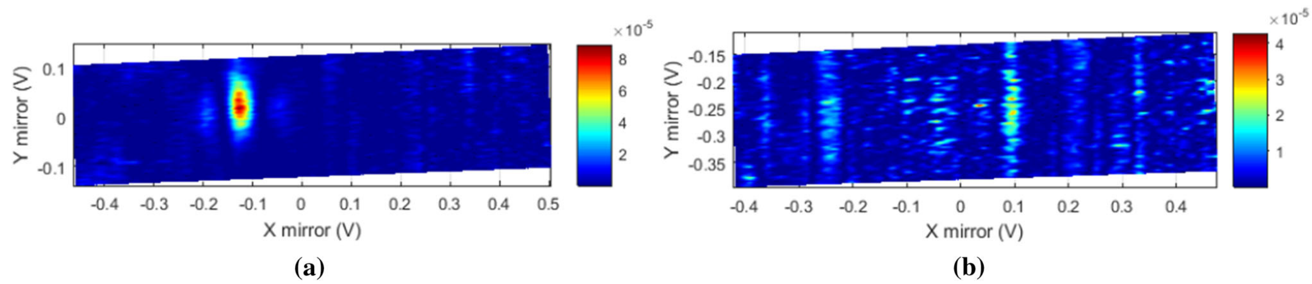

Fig. 17 Corresponding partial CDIs for scan areas **a** 1 and **b** 2 at the excitation frequency of 199.22 Hz

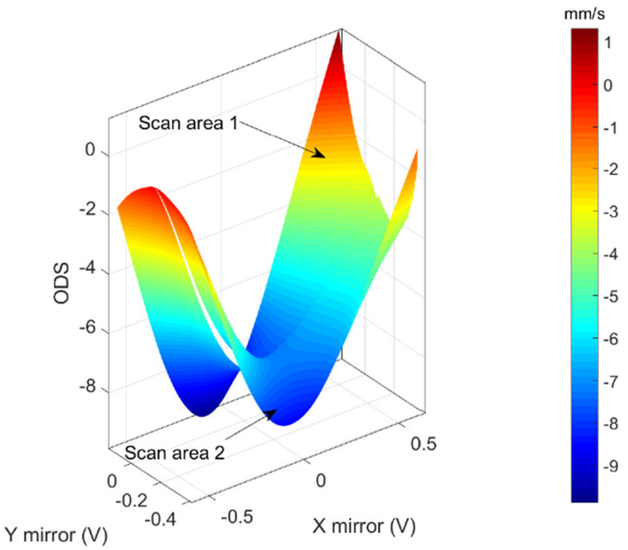

Fig. 18 Full ODS of the damaged composite plate at the excitation frequency of 297.27 Hz

in Fig. 25a and b, respectively. One can see that their shapes are more clear than those at the excitation frequencies of 29.3Hz, 82.03 Hz, and 297.27 Hz, but less clear than those at the excitation frequencies of 199.22 Hz and 563.67 Hz.

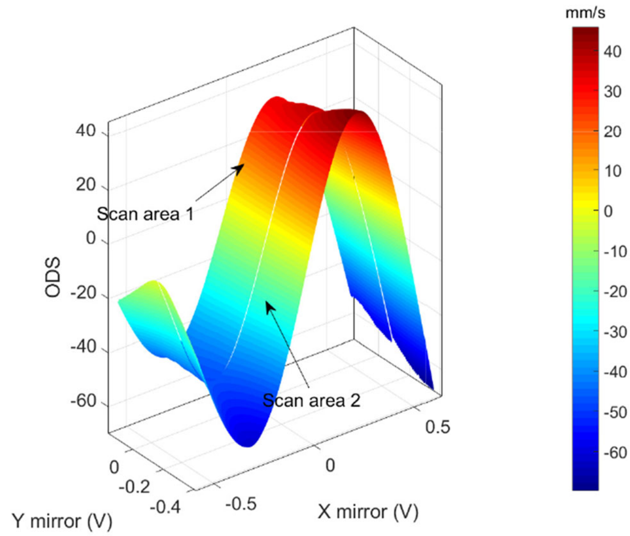

Fig. 21 Full ODS of the damaged composite plate at the excitation frequency of 563.67 Hz

Corresponding partial CDIs for scan areas 1 and 2 are shown in Fig. 26a and b, respectively. One can see that there are some scattered small areas with high CDI values in the two CDIs and none of them are at the two possible damage loca-

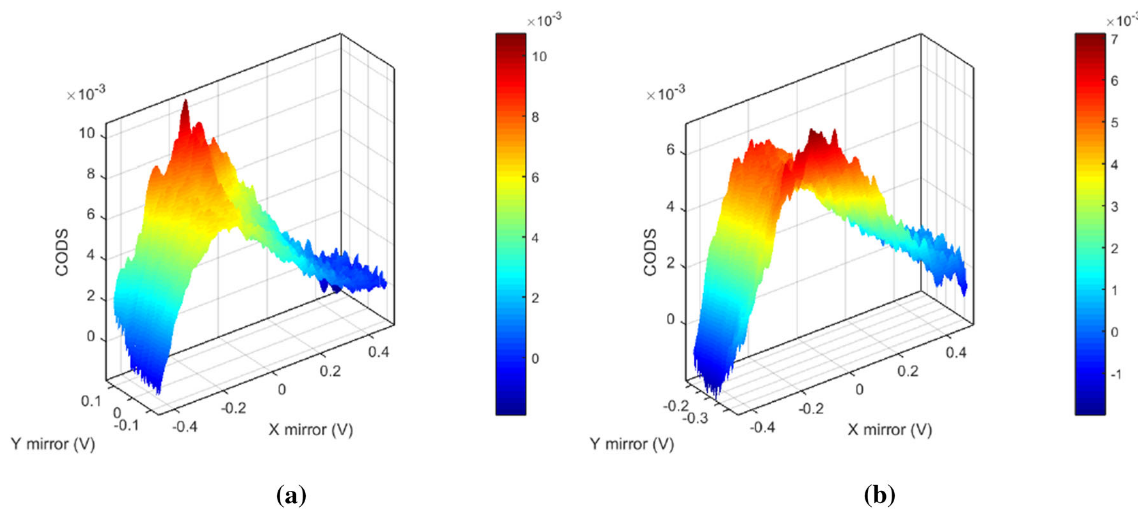

Fig. 19 Corresponding partial CODSs of scan areas **a** 1 and **b** 2 at the excitation frequency of 297.27 Hz

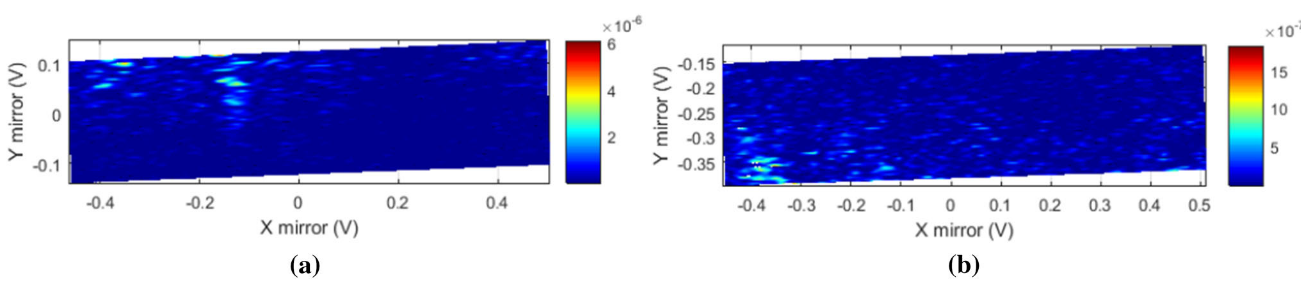

Fig. 20 Corresponding partial CDIs for scan areas **a** 1 and **b** 2 at the excitation frequency of 297.27 Hz

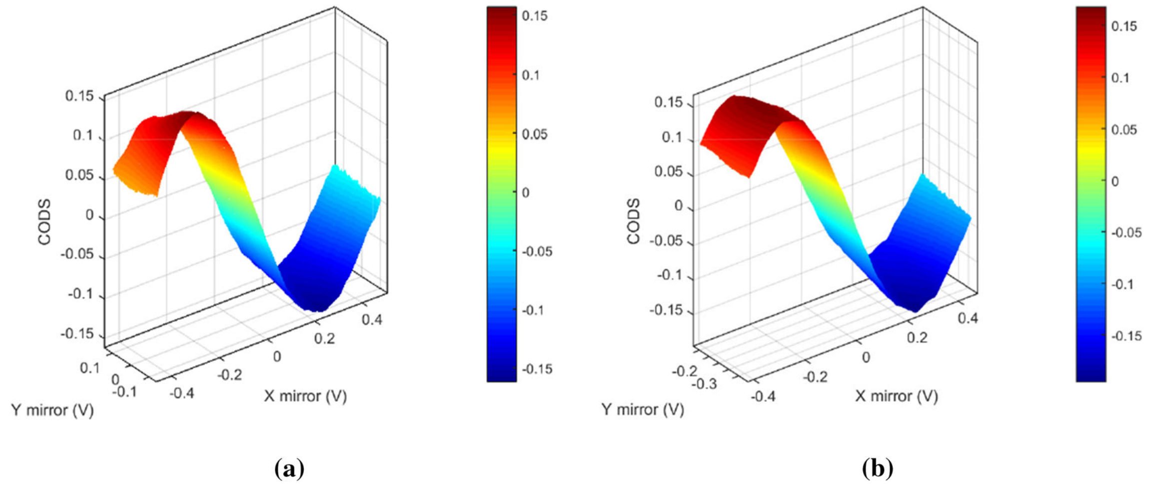

Fig. 22 Corresponding partial CODSs of scan areas **a** 1 and **b** 2 at the excitation frequency of 563.67 Hz

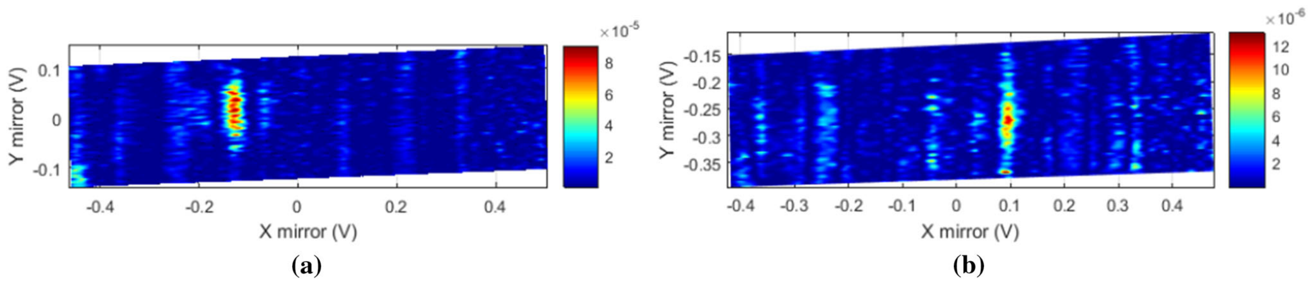

Fig. 23 Corresponding partial CDIs for scan areas **a** 1 and **b** 2 at the excitation frequency of 563.67 Hz

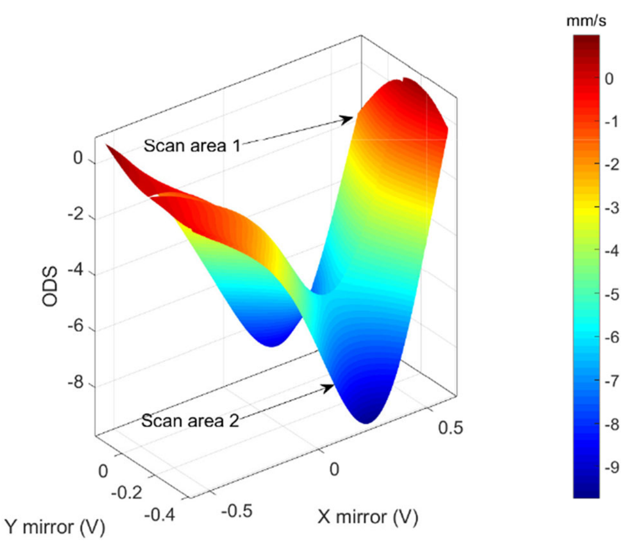

Fig. 24 Full ODS of the damaged composite plate at the excitation frequency of 1040.23 Hz

tions obtained by the CDIs at the excitation frequencies of 199.22 Hz and 563.67 Hz. Hence, the CDIs at this excitation frequency cannot be used for detection of damage locations.

3.1.7 Excitation Frequency of 1777.73 Hz

The full ODS of the damaged composite plate at the excitation frequency of 1777.73 Hz is shown in Fig. 27, which is formed by two partial ODSs corresponding to scan areas 1 and 2. One can see that the full ODS of the plate corresponding to its seventh mode is another coupled bending-bending mode along both long and short edge directions of the plate. Corresponding partial CODSs of scan areas 1 and 2 are shown in Fig. 28a and b, respectively. One can see that shapes of the CODSs are clear. Corresponding partial CDIs for scan areas 1 and 2 are shown in Fig. 29a and b, respectively. Similar to the CDIs at the excitation frequency of 1040.23 Hz, only few scattered small areas with high CDI values can be seen in the two CDIs and none of them are at the two possible damage locations obtained by the CDIs at the excitation frequencies of 199.22 Hz and 563.67 Hz. Hence, the CDIs at this excitation frequency cannot be used either for detection of damage locations.

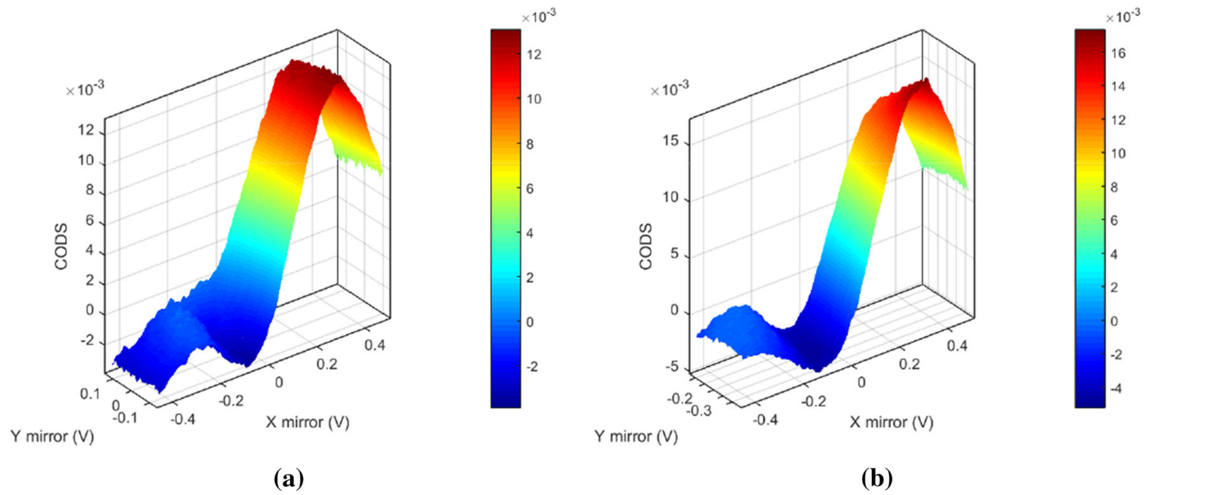

Fig. 25 Corresponding partial CODSs of scan areas **a** 1 and **b** 2 at the excitation frequency of 1040.23 Hz

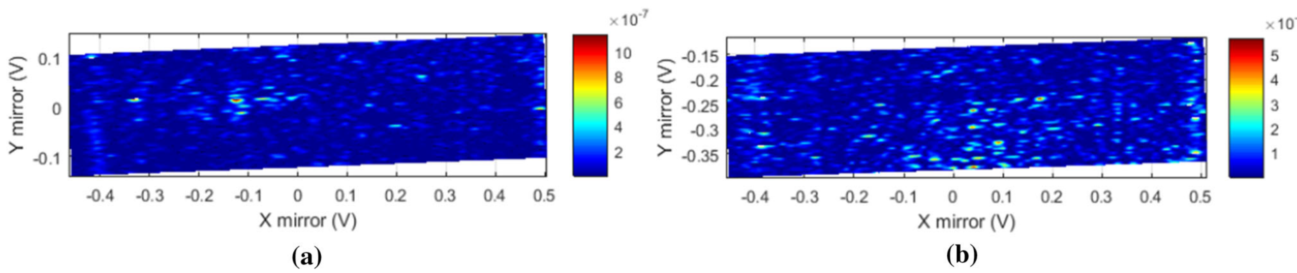

Fig. 26 Corresponding partial CDIs for scan areas **a** 1 and **b** 2 at the excitation frequency of 1040.23 Hz

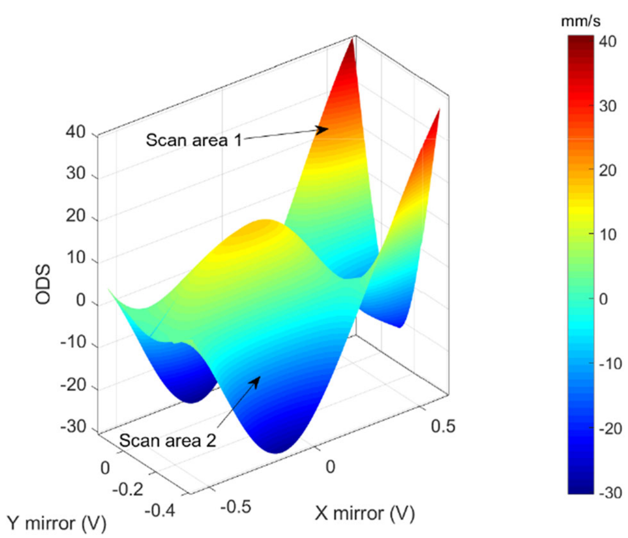

Fig. 27 Full ODS of the damaged composite plate at the excitation frequency of 1777.73 Hz

3.1.8 Summary of Results at Different Excitation Frequencies

Results using CDIs at different excitation frequencies to detect possible damage locations in the composite plate are summarized in Table 1. In the current experimental setup, the plate is excited at frequencies that are close to its natural frequencies; ODSs of the plate are close to its mode shapes, and some mode shapes of the plate are similar to mode shapes of a cantilever beam since its length is three times of its width. The third and fifth modes of the plate are pure bending modes along its long edge direction, and corresponding CODSs calculated along the long edge direction have relatively large values, as shown in Figs. 15 and 22, respectively, and consequently high signal-to-noise ratios (SNRs). Hence, they are the most beneficial modes for detecting the two damage. It is not easy to detect damage of the small-sized and stiff plate here using its first and second modes, since corresponding CODSs calculated along the long edge direction have relatively small values, as shown in Figs. 8 and 12, respectively, and consequently low SNRs. The fourth and sixth modes of the plate are coupled bending-bending modes along its long and short edge directions. Since the length of the plate is much larger than its width and the scan trajectory is along its long edge direction, CODSs corresponding to the fourth and sixth modes are also calculated along the long edge direction, which have relatively small values, as shown in Figs. 19 and 25, respectively, and consequently low SNRs. Hence, CODSs corresponding to the fourth and sixth modes cannot be used

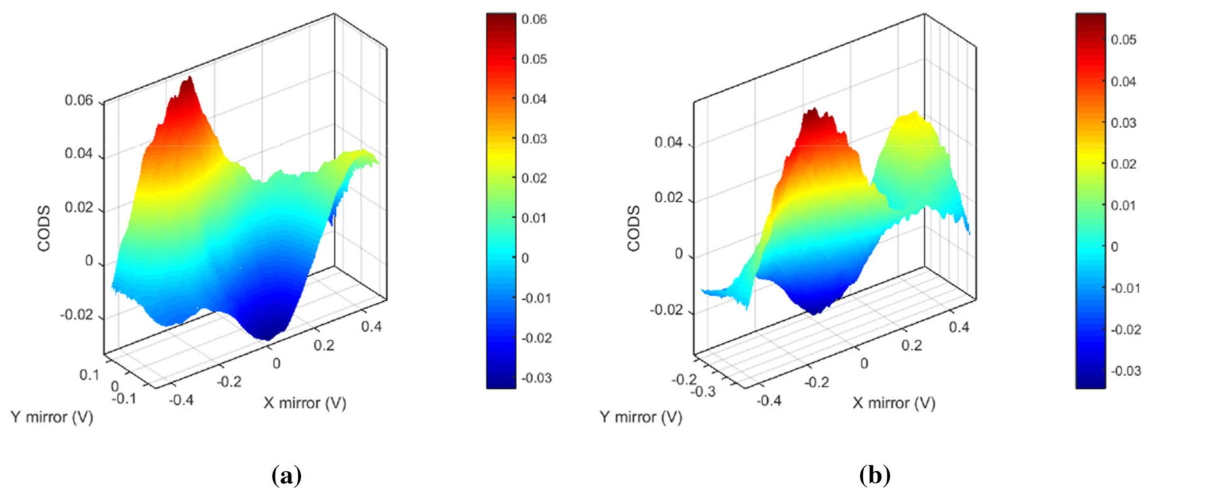

Fig. 28 Corresponding partial CODSs of scan areas **a** 1 and **b** 2 at the excitation frequency of 1777.73 Hz

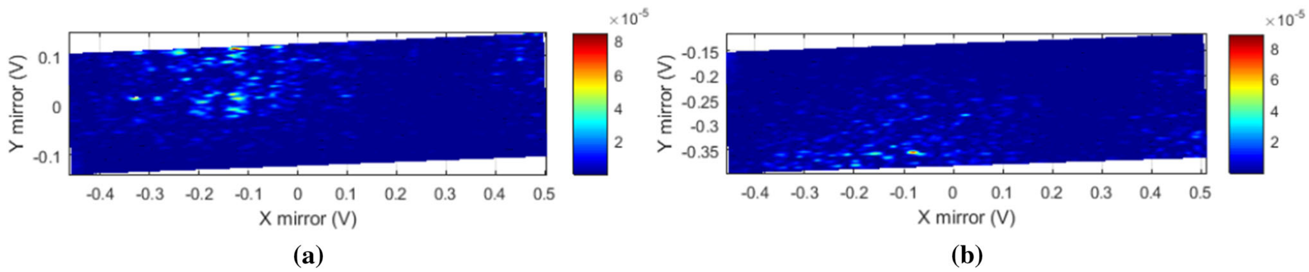

Fig. 29 Corresponding partial CDIs for scan areas **a** 1 and **b** 2 at the excitation frequency of 1777.73 Hz

Table 1 Summary of detection results at different excitation frequencies

Frequency (Hz)	Mode	Detection
29.3	Pure bending mode along long edge	No
82.03	Pure bending mode along the long	No
199.22	Pure bending mode along long edge	Yes
297.27	Coupled bending-bending mode	No
563.67	Pure bending mode along long edge	Yes
1040.23	Coupled bending-bending mode	No
1777.73	Coupled bending-bending mode	No

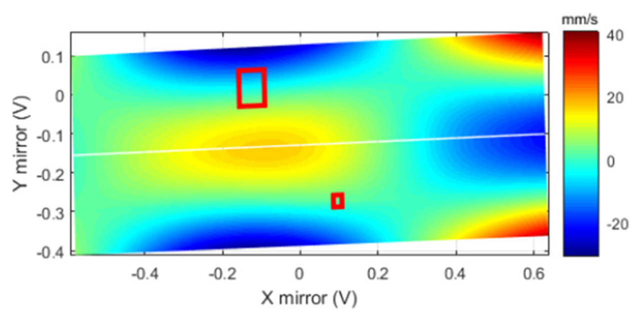

Fig. 30 Two possible damage locations on the full ODS of the damaged composite plate at the excitation frequency of 1040.23 Hz

to detect the two damage. The two damage locations of the plate are close to nodal lines of the seventh mode of the plate, as shown in Fig. 30, which causes the corresponding CODS insensitive to the local anomaly induced by the two damage.

Based on the above results, normalized average CDIs for scan areas 1 and 2 are calculated using the CDIs at the excitation frequencies of 199.22 Hz and 563.67 Hz, as shown in Fig. 31a and b, respectively. From the normalized average CDIs, one can see that there is two damage in the composite plate, which is consistent with the prescribed number of damage. Estimated locations of the two damage are obtained by the following procedure. First, input voltages of the X and Y mirrors corresponding to the maximum normalized average CDI value in either damage are extracted. Second, the laser spot is directed to a point with the input voltages obtained in the first step and this point is assumed as the center of the damage. Sizes of the two damage are also estimated by a similar procedure. Comparison between estimated and prescribed damage locations and sizes of the two damage is shown in Fig. 32. One can see that the estimated locations of the two damage are in good agreement with the prescribed damage locations. The two damage is named damage 1 and damage 2 hereafter. Prescribed and estimated sizes of damage 1

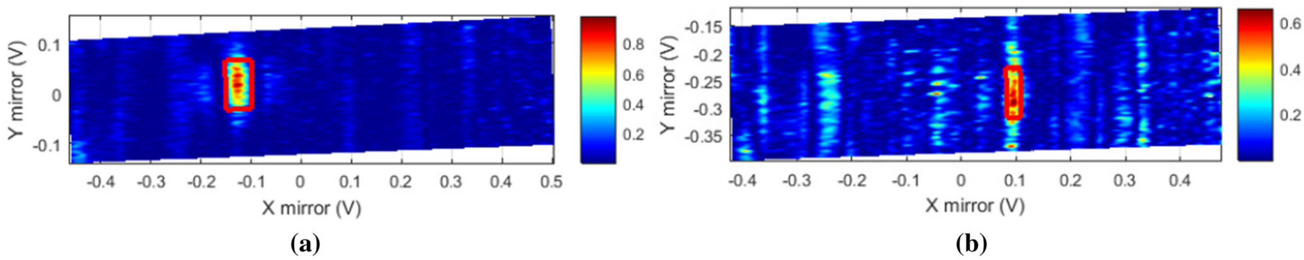

Fig. 31 Normalized average CDIs for scan areas **a** 1 and **b** 2 using the CDIs at the excitation frequencies of 199.22 Hz and 563.67 Hz. The estimated size of either damage is indicated by a rectangular in solid lines

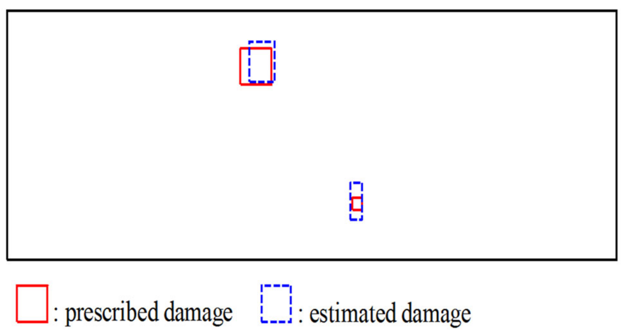

Fig. 32 Comparison between estimated and prescribed locations and sizes of the two damage

are 15 mm × 15 mm and 12 mm × 16 mm, respectively. Prescribed and estimated sizes of damage 2 are 5 mm × 5 mm and 6 mm × 15 mm, respectively. One can see that the estimated size of damage 1 is in good agreement with the prescribed size. However, the size of damage 2 is overestimated in the short edge direction of the plate. Possible reasons are that the prescribed size of damage 2 is only 5 mm × 5 mm and stiffness of the plate is much higher along the short edge direction. Hence, it can be difficult to achieve a high SNR in this direction.

The above damage detection results are obtained by dividing the damaged composite plate into two scan areas and using the maximum hardware storage ability of the CSLDV.

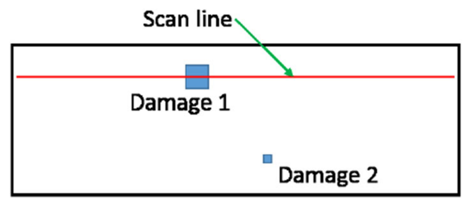

Fig. 34 Scan line assigned to go through the center of damage 1

One can also treat the whole plate as one scan area and use only one 2D scan trajectory. CDIs of the plate using only one full scan at the excitation frequencies of 199.22 Hz and 563.67 Hz are shown in Fig. 33a and b, respectively. One can see that damage 1 with the prescribed size of 15 mm × 15 mm can be clearly detected with only one full scan. However, damage 2 with the prescribed size of 5 mm × 5 mm is not detected, since spatial resolution of a full ODS of the plate with only one whole scan area is half of that of the full ODS with two partial scan areas, which makes it more difficult to capture the local anomaly induced by damage 2.

3.2 Effects of the Scan Frequency and Number of Multiple Scans on ODSs, CODSs, and CDIs

When a CSLDV is used for damage detection, an important point is to choose a suitable scan frequency f_{scan}. This is especially essential when the CSLDV is used for small-sized

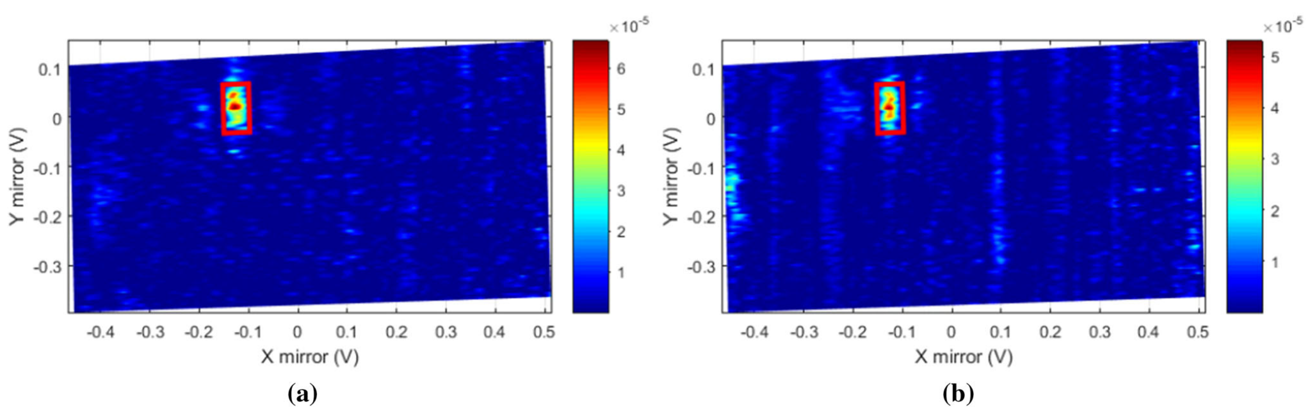

Fig. 33 CDIs of the damaged composite plate with only one full scan at the excitation frequencies of **a** 199.22 Hz and **b** 563.67 Hz. The estimated size of damage 1 is indicated by a rectangular in solid lines

Table 2 Four combinations of f_{scan} and M

Combination	f_{scan} (Hz)	M
1st	0.05	11
2nd	0.25	51
3rd	0.5	101
4th	1	201

damage detection. If the scan frequency is high, the laser spot quickly sweeps each point on a structure surface and may not be able to capture small local anomaly induced by damage. In order to improve SNRs, Chen et al. [26] proposed an averaging technique and suggested that the number of multiple scans M for a scan line be large to reduce the adverse effect of measurement noise on damage detection. Hence, the number of multiple scans is another factor that needs to be considered. Since the scan time of one whole scan is fixed by hardware, a lower scan frequency is associated with a smaller number of multiple scans while a higher scan frequency is associated with a larger number of multiple scans. In order to investigate which factor plays a more important role in damage detection, a scan line is assigned to go through the center of damage 1, as shown in Fig. 34. The scan time is fixed at 100 s and four combinations of f_{scan} and M are used, as shown in Table 2. Periodic triangular signals corresponding to different f_{scan} and a constant signal are given to the X and Y mirrors, respectively, to achieve the line scan. ODSs, CODSs, and CDIs along the scan line at the excitation frequencies of 199.22 Hz and 563.67 Hz are shown in Figs. 35, 36, and 37, respectively. One can see that the ODSs are in good agreement with different combinations of f_{scan} and M, which indicates that an ODS does not have preference on the scan frequency and number of multiple scans. One can see in Fig. 36a with the excitation frequency of 199.22 Hz that the CODSs are in good agreement in the first three combinations of f_{scan} and M. However, in the fourth combination with the scan frequency being 1 Hz and $M = 201$, the CODS at the right boundary of the scan line has abrupt change. Similar abrupt change can be seen in the CODS in Fig. 36b in the fourth combination of f_{scan} and M at the excitation frequency of 563.67 Hz. The reason is that the scan direction quickly changes at two ends of the scan line when the scan frequency is high. This abrupt change leads to high CDI values at the right boundary of the corresponding CDI shown in Fig. 37, which can have an adverse effect on damage detection. One can see that the CDI in Fig. 37b in the fourth combination cannot be used to detect damage 1.

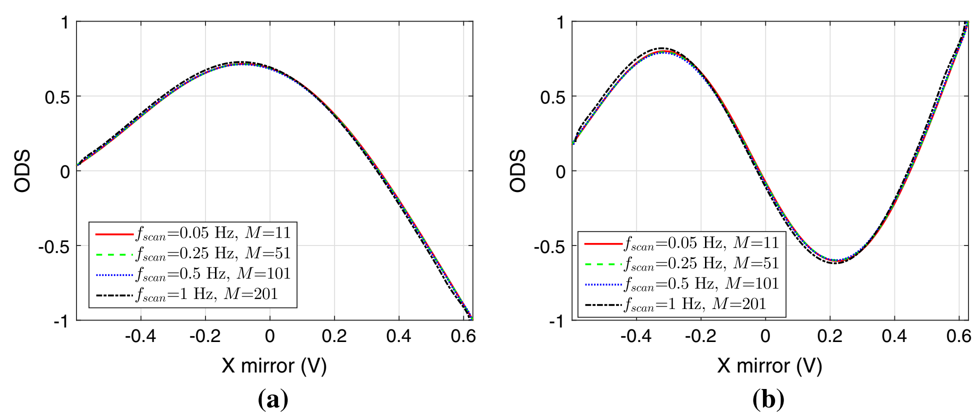

Fig. 35 ODSs with four different combinations of f_{scan} and M at the excitation frequencies of **a** 199.22 Hz and **b** 563.67 Hz

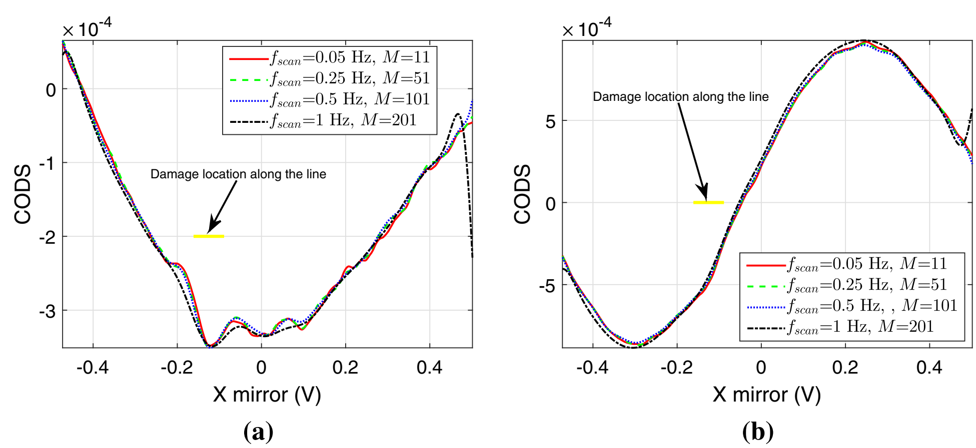

Fig. 36 CODSs with four different combinations of f_{scan} and M at the excitation frequencies of **a** 199.22 Hz and **b** 563.67 Hz

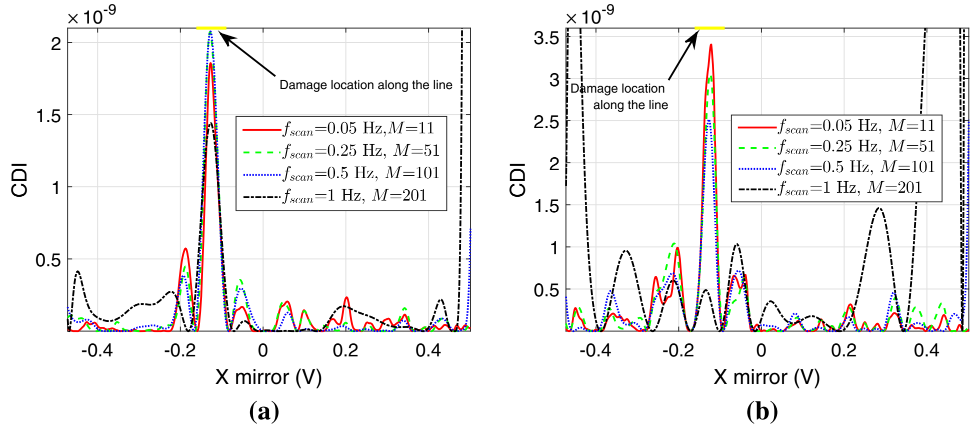

Fig. 37 CDIs with four different combinations of f_{scan} and M at the excitation frequencies of **a** 199.22 Hz and **b** 563.67 Hz

Hence, a CODS and a CDI prefer a low scan frequency to a large number of multiple scans.

4 Conclusion

A CSLDV and a curvature-based damage detection method are successfully applied in this work to detect two hidden delamination damage in a composite plate in a round robin study. Non-contact excitation and response measurement are achieved by a speaker and the CSLDV, respectively. Dense spatial resolution of ODSs, CODSs, and CDIs of the plate at seven excitation frequencies is obtained. The CODSs corresponding to the first two modes of the plate do not have as good quality as those corresponding to higher-order modes. The CODSs corresponding to the third and fifth modes that are pure bending modes along the long edge direction of the plate are most sensitive to local anomaly induced by the two damage. Hence, for detection of damage in a composite plate with a relatively large aspect ratio with use of a CSLDV, it is recommended to first conduct a simulation study to obtain its mode shapes and use excitation frequencies corresponding to pure bending modes along the long edge direction of the plate for further experimental investigation. While only the damage with the prescribed size of 15 mm × 15 mm is detected when applying only one full scan to the damaged composite plate, both of the two damage is detected when the plate is divided into two partial scan areas since spatial resolution of a full ODS of the plate in this case is twice that with only one full scan; this increases the probability to capture the anomaly induced by the two damage. Hence, denser spatial resolution of an ODS is beneficial for damage detection and it is recommended to divide a composite plate with a relatively large area into two or more scan areas along the long edge direction of the plate. The accuracy and sensitivity of a CSLDV used for detection of hidden damage in a composite plate are fully investigated in this round robin study and locations and sizes of the two damage are well estimated with use of the CSLDV due to its two advantages, i.e., dense measurement and an advanced damage detection method. Based on the feedback from the organizer of the round robin study, locations of the two damage in the composite plate are only detected by the authors with use of a CSLDV in this round robin study.

Acknowledgements The authors would like to thank Dr. Dario Di Maio for organizing this round robin study and manufacturing the composite plate. They are also grateful for the financial support from the National Science Foundation through Grant Numbers CMMI-1229532, CMMI-1335024, CMMI-1763024, and CMMI-1762917 and College of Engineering and Information Technology at the University of Maryland, Baltimore County through a Strategic Plan Implementation Grant.

References

1. Hull, D., Clyne, T.W.: An Introduction to Composite Materials. Cambridge University Press, Cambridge (1996)
2. Zou, Y., Tong, L., Steven, G.P.: Vibration-based model-dependent damage (delamination) identification and health monitoring for composite structures: a review. J. Sound Vib. **230**(2), 357–378 (2000)
3. Doebling, S.W., Farrar, C.R., Prime, M.B., et al.: A summary review of vibration-based damage identification methods. Shock Vib. Dig. **30**(2), 91–105 (1998)
4. Fan, W., Qiao, P.: Vibration-based damage identification methods: a review and comparative study. Struct. Health Monit. **10**(1), 83–111 (2011)
5. Valdes, S.D., Soutis, C.: Delamination detection in composite laminates from variations of their modal characteristics. J. Sound Vib. **228**(1), 1–9 (1999)
6. Qiao, P., Lestari, W., Shah, M.G., Wang, J.: Dynamics-based damage detection of composite laminated beams using contact and noncontact measurement systems. J. Compos. Mater. **41**(10), 1217–1252 (2007)
7. Qiao, P., Lu, K., Lestari, W., Wang, J.: Curvature mode shape-based damage detection in composite laminated plates. Compos. Struct. **80**(3), 409–428 (2007)
8. Lestari, W., Qiao, P., Hanagud, S.: Curvature mode shape-based damage assessment of carbon/epoxy composite beams. J. Intell. Mater. Syst. Struct. **18**(3), 189–208 (2007)

9. He, M., Yang, T., Du, Y.: Nondestructive identification of composite beams damage based on the curvature mode difference. Compos. Struct. **176**, 178–186 (2017)
10. Yam, L., Yan, Y., Jiang, J.: Vibration-based damage detection for composite structures using wavelet transform and neural network identification. Compos. Struct. **60**(4), 403–412 (2003)
11. Katunin, A.: Damage identification in composite plates using two-dimensional b-spline wavelets. Mech. Syst. Signal Process. **25**(8), 3153–3167 (2011)
12. Katunin, A., Przystałka, P.: Damage assessment in composite plates using fractional wavelet transform of modal shapes with optimized selection of spatial wavelets. Eng. Appl. Artif. Intell. **30**, 73–85 (2014)
13. Rucka, M., Wilde, K.: Application of continuous wavelet transform in vibration based damage detection method for beams and plates. J. Sound Vib. **297**(3–5), 536–550 (2006)
14. Fan, W., Qiao, P.: A 2-d continuous wavelet transform of mode shape data for damage detection of plate structures. Int. J. Solids Struct. **46**(25), 4379–4395 (2009)
15. Cornwell, P., Doebling, S.W., Farrar, C.R.: Application of the strain energy damage detection method to plate-like structures. J. Sound Vib. **224**(2), 359–374 (1999)
16. Yoon, M., Heider, D., Gillespie, J., Ratcliffe, C., Crane, R.: Local damage detection using the two-dimensional gapped smoothing method. J. Sound Vib. **279**(1), 119–139 (2005)
17. Yang, C., Oyadiji, S.O.: Delamination detection in composite laminate plates using 2d wavelet analysis of modal frequency surface. Comput. Struct. **179**, 109–126 (2017)
18. Xu, W., Cao, M., Li, X., Radzieński, M., Ostachowicz, W., Bai, R.: Delamination monitoring in cfrp laminated plates under noisy conditions using complex-wavelet 2d curvature mode shapes. Smart Mater. Struct. **26**(10), 104008 (2017)
19. Rothberg, S., Allen, M., Castellini, P., Di Maio, D., Dirckx, J., Ewins, D., Halkon, B.J., Muyshondt, P., Paone, N., Ryan, T., et al.: An international review of laser Doppler vibrometry: making light work of vibration measurement. Opt. Lasers Eng. **99**, 11–22 (2017)
20. Castellini, P., Martarelli, M., Tomasini, E.: Laser Doppler vibrometry: development of advanced solutions answering to technology's needs. Mech. Syst. Signal Process. **20**(6), 1265–1285 (2006)
21. Di Maio, D., Ewins, D.: Continuous scan, a method for performing modal testing using meaningful measurement parameters; part i. Mech. Syst. Signal Process. **25**(8), 3027–3042 (2011)
22. Pandey, A., Biswas, M., Samman, M.: Damage detection from changes in curvature mode shapes. J. Sound Vib. **145**(2), 321–332 (1991)
23. Xu, W., Cao, M., Ostachowicz, W., Radzieński, M., Xia, N.: Two-dimensional curvature mode shape method based on wavelets and teager energy for damage detection in plates. J. Sound Vib. **347**, 266–278 (2015)
24. Sriram, P., Craig, J.: Of technology. Int. J. Anal. Exp. Modal Anal. **7**(3), 169–178 (1992)
25. Stanbridge, A., Ewins, D.: Modal testing using a scanning laser Doppler vibrometer. Mech. Syst. Signal Process. **13**(2), 255–270 (1999)
26. Chen, D.-M., Xu, Y., Zhu, W.: Experimental investigation of notch-type damage identification with a curvature-based method by using a continuously scanning laser Doppler vibrometer system. J. Nondestruct. Eval. **36**(2), 38 (2017)
27. Xu, Y., Chen, D.-M., Zhu, W.: Damage identification of beam structures using free response shapes obtained by use of a continuously scanning laser Doppler vibrometer system. Mech. Syst. Signal Process. **92**, 226–247 (2017)
28. Chen, D.-M., Xu, Y., Zhu, W.: Identification of damage in plates using full-field measurement with a continuously scanning laser Doppler vibrometer system. J. Sound Vib. **422**, 542–567 (2018)
29. Chen, D.-M., Zhu, W.D.: Investigation of three-dimensional vibration measurement by a single scanning laser Doppler vibrometer. J. Sound Vib. **387**, 36–52 (2017)
30. dos Santos, J.A., Lopes, H., Vaz, M., Soares, C.M., Soares, C.M., De Freitas, M.: Damage localization in laminated composite plates using mode shapes measured by pulsed tv holography. Compos. struct. **76**(3), 272–281 (2006)
31. Polimeno, U., Meo, M.: Detecting barely visible impact damage detection on aircraft composites structures. Compos. Struct. **91**(4), 398–402 (2009)